

MeshCNN: A Network with an Edge

RANA HANOCKA, Tel Aviv University

AMIR HERTZ, Tel Aviv University

NOA FISH, Tel Aviv University

RAJA GIRYES, Tel Aviv University

SHACHAR FLEISHMAN, Amazon

DANIEL COHEN-OR, Tel Aviv University

A polygonal mesh representation provides an efficient approximation for 3D shapes. It explicitly captures both shape surface and topology, and leverages non-uniformity to represent large flat regions as well as sharp, intricate features. This non-uniformity and irregularity, however, inhibits mesh analysis efforts using neural networks that combine convolution and pooling operations. In this paper, we utilize the unique properties of the mesh for a direct analysis of 3D shapes using *MeshCNN*, a convolutional neural network designed specifically for triangular meshes. Analogous to classic CNNs, MeshCNN combines specialized convolution and pooling layers that operate on the mesh edges, by leveraging their intrinsic geodesic connections. Convolutions are applied on edges and the four edges of their incident triangles, and pooling is applied via an edge collapse operation that retains surface topology, thereby, generating new mesh connectivity for the subsequent convolutions. MeshCNN learns which edges to collapse, thus forming a task-driven process where the network exposes and expands the important features while discarding the redundant ones. We demonstrate the effectiveness of our task-driven pooling on various learning tasks applied to 3D meshes.

1 INTRODUCTION

Three dimensional shapes are front and center in the field of computer graphics, but also a major commodity in related fields such as computer vision and computational geometry. Shapes around us, and in particular those describing natural entities, are commonly composed of continuous surfaces.

For computational reasons, and to facilitate data processing, various discrete approximations for 3D shapes have been suggested and utilized to represent shapes in an array of applications. A favorite of many, the polygonal mesh representation, or, mesh, for short, approximates surfaces via a set of 2D polygons in 3D space [Botsch et al. 2010]. The mesh provides an efficient, non-uniform representation of the shape. On the one hand, only a small number of polygons are required to capture large, simple, surfaces. On the other, representation flexibility supports a higher resolution when needed, allowing a faithful reconstruction, or portrayal, of salient shape features that are often geometrically intricate. Another lucrative characteristic of the mesh is its native provision of connectivity information. This helps painting a complete picture of the underlying structure, forming an overall better approximation of the shape.

These advantages are apparent in comparison to another popular option - the point cloud representation. Despite its simplicity and direct relation to common data acquisition techniques (scanning), the point cloud representation falls short in many scenarios, where higher quality and preservation of sharp shape features are required (for example, see Figure 7).

Convolutional neural networks (CNNs) are a form of deep neural networks, where convolution operations are combined to aid in the learning of spatial features in the data. CNNs rose to fame in recent years, demonstrating outstanding performance on popular tasks such as image classification and semantic segmentation [Chen et al. 2018; Sermanet et al. 2013; Simonyan and Zisserman 2014].

Following their success in the image domain, extensions to the 3D domain were quickly made, with shapes represented and processed predominately in voxel [Li et al. 2017; Wu et al. 2015] or point cloud form [Qi et al. 2017b]. Voxel representations are grid-based, thus 3D convolutions are an easy fit, but the transition from image to volume adds another spatial dimension, and memory requirements become prohibitively large. Additionally, sparsity of shape occupancy within the volume leads to wasteful computations of empty convolutions. Point-based approaches benefit from a compact representation of the input, but are inherently oblivious to the local surface, and, moreover, due to ordering ambiguity, the notion of point neighborhood and connectivity is ill-defined and the application of convolution and pooling operations is non-trivial.

Aiming to tap into the natural potential of the native mesh representation, we present *MeshCNN* - a neural network that is analogous to the well-known CNN, but designed specifically for meshes. MeshCNN operates directly on meshes, and performs convolution and pooling operations that are adapted to their properties. In

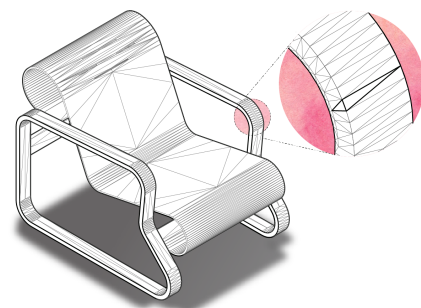


Fig. 1. Meshes enable a non-uniform representation which adapts to the given geometry: large flat regions can be represented by a small number of large polygons, with detailed non-smooth regions represented by a larger number of small polygons. By operating on mesh edges, MeshCNN enjoys a consistent setting of well-defined neighborhoods for convolution and pooling, where each edge has four neighboring edges dictated by the two faces it is incident to.

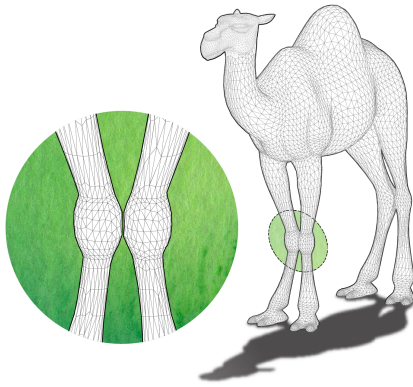


Fig. 2. An example highlighting the contribution of the mesh representation to the correct understanding of shape structure. The front leg joints of the camel (as shown in the zoom-in) are articulated such that they are almost, but not quite, touching one another. Despite the Euclidean proximity, the mesh, unlike the point cloud, is able to easily convey their distinct identities through geodesic separation.

MeshCNN, the edges of a mesh are analogous to pixels in an image, as they are the basic building blocks upon which all operations are applied. The edge set is attractive in its characteristic consistent ordering. Every edge has exactly four adjacent edges that can be traversed and extracted to form convolutional neighborhoods of elements for proper filter application and feature computation (illustration in Figure 1 & 4).

A key feature of MeshCNN is the special task-driven pooling operation, *mesh pooling*. This operation is based on the well-known mesh simplification technique *edge collapse* [Hoppe 1997], but, where conventional edge collapse aims to minimize the introduced geometric distortion by retaining edges with geometric saliency, mesh pooling delegates the choice of which edges to collapse to the network: resulting in a task-specific purging of edges whose contribution to the minimization of the current objective is minor. See examples in Figure 8 and 3.

2 RELATED WORKS

Many of the operators that we present or use in our work are based on classic mesh processing techniques [Botsch et al. 2010], or more specifically, mesh simplification techniques [Garland and Heckbert 1997; Hoppe 1997; Hoppe et al. 1993]. In particular, we use the edge-collapse technique [Hoppe 1997] for our task-driven pooling operator.

Data analysis using neural networks has been widely explored in recent years. Major performance improvements reported on popular analysis tasks of 2D data (images) have spurred a natural extension to the 3D domain. In this section, we revisit relevant work on 3D data analysis using neural networks, organized according to input representation type.

Multi-view 2D projections. Leveraging existing techniques and architectures from the 2D domain is made possible by representing 3D shapes through their 2D projections from various viewpoints.

These sets of rendered images serve as input to subsequent processing by standard CNN models. Su et al. [2015] followed this paradigm, and trained a classification network to determine shape class. Qi et al. [2016] explored both view-based and volumetric approaches, and observed the superiority of the first.

Volumetric. Transforming a 3D shape into binary voxel form provides a grid-based representation that is analogous to the 2D grid of an image. As such, operations that are applied on 2D grids can be extended to 3D grids in a straight-forward manner, thus allowing a natural transference of common image-based approaches to the shape domain. Wu et al. [2015] pioneered this concept, and presented a CNN that processes voxelized shapes for classification and completion. Following that, Brock et al. [2016] tackled shape reconstruction using a voxel-based variational autoencoder, and Tchapmi et al. [2017] combined trilinear interpolation and Conditional Random Fields (CRF) with a volumetric network to promote semantic shape segmentation. Hanocka et al. [2018] used volumetric shape representations to train a network to regress grid-based warp fields for shape alignment, and applied the estimated deformation on the original mesh. Despite their alluring simplicity, volumetric representations are computationally demanding, requiring significant memory usage. To alleviate this, several acceleration strategies have been proposed, where sparsity of shape occupancy within the volume is exploited for representation reduction [Graham et al. 2017; Li et al. 2016; Riegler et al. 2017; Wang et al. 2017]

Graph. A common generalization of grid-based representations that allows non-regularity, is the graph structure. To support graph-based data analysis, considerable focus has been directed toward the application of neural networks to popular tasks involving data represented in graph form, mainly, social networks, sensor networks in communication, or genetic data. One approach advocates for the processing of the Laplacian of the graph representation [Bruna et al. 2014; Henaff et al. 2015], and thus operates in the spectral domain. Another approach opts to process the graph directly by extracting locally connected regions and transforming them into a canonical form to be processed by a neural network [Niepert et al. 2016]. Atwood et al. [2016] proposed diffusion-convolution, where diffusion is applied on each node to determine its local neighborhood. Such et al. [2017] introduced the concept of vertex filtering on graphs, but did not incorporate pooling operations for feature aggregation.

Manifold. The pioneering work of Masci et al. [2015] introduced deep learning of local features on meshes, and has shown how to use these learned features for correspondence and retrieval. Often, local patches on a manifold shape are approximately Euclidean. This characteristic can be exploited for manifold shape analysis using standard CNNs, by parameterizing the 3D manifold to 2D [Boscaini et al. 2016; Henaff et al. 2015; Maron et al. 2017; Sinha et al. 2016]. See [Bronstein et al. 2017] for a comprehensive survey. These methods are robust to isometric deformations on shapes, but are less suitable for classes describing man-made objects, which commonly contain large flat regions and sharp features.

Tatarchenko et al. [2018] introduce tangent convolution, where a small neighborhood around each point is used to reconstruct the local function upon which convolution is applied. Differently from previous work, pooling operations are incorporated in this work, and performed by subsampling on a regular 3D grid.

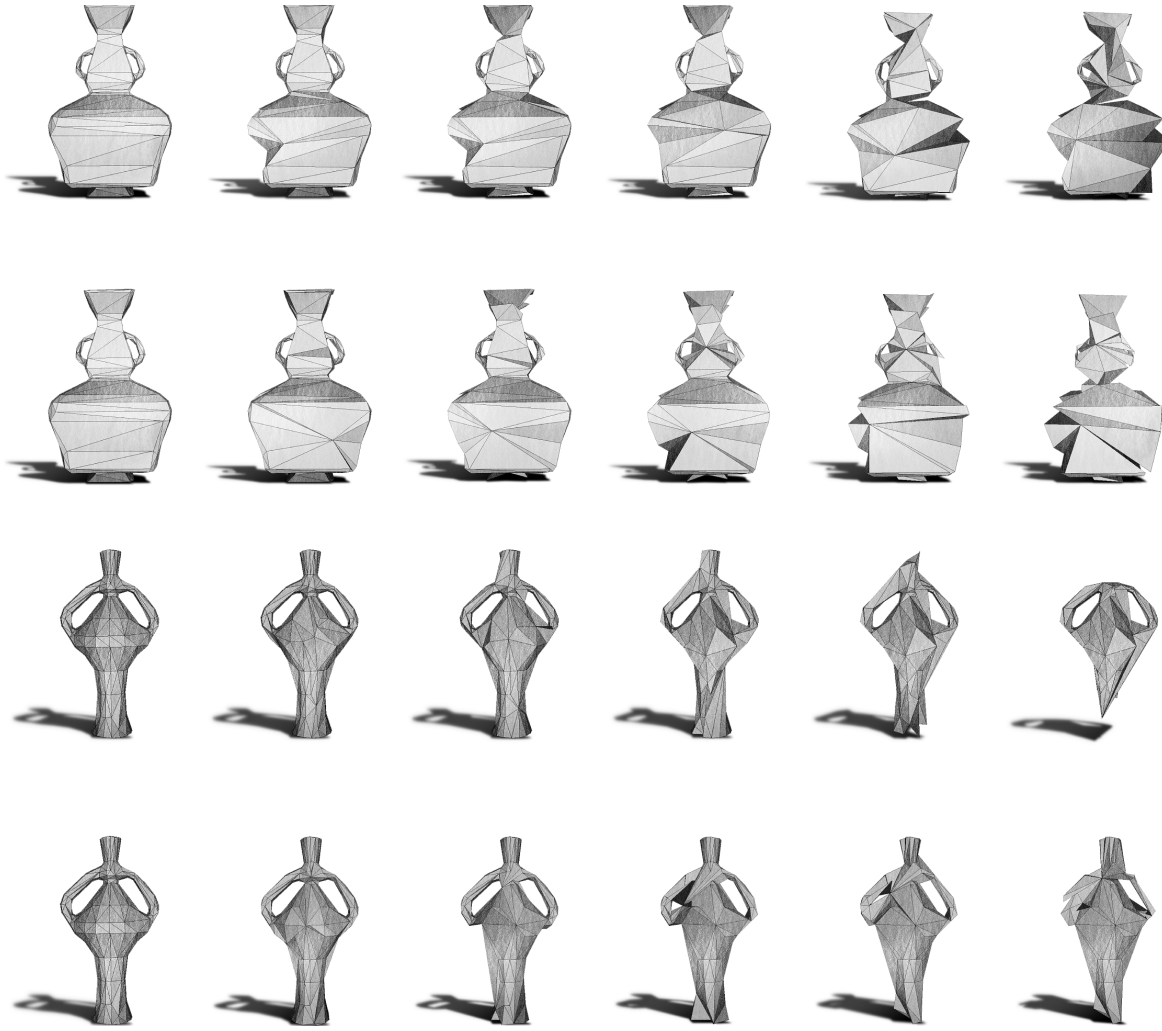


Fig. 3. Pooling on learned edge features allows MeshCNN to determine which parts of the mesh to simplify. Unlike a geometric simplification (which computes the geometric distortion of removing each edge), MeshCNN learns which edge to collapse based on the task. The top row is the intermediate simplification results on training a network to classify whether vases have a handle or not vs. the bottom row, which is the result of training a network to classify whether a vase has a neck (top piece) or not.

Point clouds. Arguably the simplest of all representations, the point cloud representation provides a no-frills approximation for an underlying 3D shape. The close relationship to data acquisition, and ease of conversion from other representations, make the point cloud form a classic candidate for data analysis. Accordingly, recent effort has focused on developing techniques for point cloud shape analysis using neural networks. PointNet [Qi et al. 2017b] propose using 1×1 convolutions followed by global max pooling for order invariance. In its followup work - PointNet++ [Qi et al. 2017], points are partitioned to capture local structures better. Wang et al. [2018] take into account local point neighborhood information, and perform dynamic updates driven by similarity calculation between points based on distance in feature space.

Recently, Li et al. [2018] presented PointCNN, which extends the notion of convolution from a local grid to an Ξ -convolution on a local set of points. The local features that are encoded per point are influenced by the points residing in its Euclidean neighborhood. In our work, we rely on mesh edges to provide non-uniform, geodesic neighborhood information. Subsequently, feature computation is performed on top of the edges themselves, while leveraging mesh decimation techniques, such as edge collapse, in a manner that adheres to shape geometry and topology.

3 OVERVIEW: APPLYING CNN ON MESHES

Polygonal meshes are the most fundamental and commonly used 3D data representation in computer graphics. A mesh explicitly represents both the geometry and topology of a surface. It provides

direct access to geodesic neighborhood information, faithfully describing intricate surface structures while disambiguating Euclidean proximity from on-surface, geodesic proximity (see Figure 2). Furthermore, the mesh administers a non-uniform representation that is adaptable to the underlying shape geometry. Large flat regions can be represented by a small number of large polygons, with a larger number of flexibly sized polygons covering detailed, non-smooth regions (see Figure 1). This agility of the mesh reflects directly upon its effectiveness as a representation, and is apparent by simply considering its inherent ability to capture sharp shape features common in man-made 3D objects, as opposed to point set representations that struggle under these conditions.

Realizing our goal to apply the CNN paradigm directly onto triangular meshes, necessitates an analogous definition and implementation of the standard operators that are the backbone of every CNN. Image-based CNNs contain convolutional, non-linearity and simplification (pooling) layers within their pipeline, a combination which results in a robust learning framework. As opposed to images which are represented on a regular grid of discrete values, the key challenge in mesh analysis is its inherent irregularity and non-uniformity.

In our work, we aim to exploit these challenging and unique properties, rather than bypassing them. Accordingly, we design our network to deliberately apply convolution and pooling operations directly on the constructs of the mesh, and avoid resampling or conversion to a regular and uniform representation. While image-based CNNs are often restricted to predetermined input dimensions, a notable advantage of the nature of our simplification, which is a mesh-based simplification using edge collapse, is that it provides flexibility with regards to the output dimensions of the pooling layer. In other words, an arbitrarily sized mesh given as input to the network, is simplified by the pooling layers in a dynamic manner, such that the desired resolution is reached before proceeding to the final fully connected layers. As this resolution highly influences the capacity and computational complexity of the network, it should be adjusted appropriately.

Our network operates and learns features on the edges of the mesh, as they form a consistent and stable set of entities, despite the overall irregular nature of the mesh. Each edge is adjacent to two triangles (faces), defining a natural, fixed-sized neighborhood of edges (see Figure 4(a), where the red edge has 4 neighboring edges shown in blue). Such an edge neighborhood forms a receptive field with which the **convolution** learnable filters are multiplied. The **pooling** operation is accomplished by an edge collapse process, as demonstrated in Figure 4 (b) and (c). In (b), the dashed edge is collapsing to a point, and, subsequently, the four incident edges (blue) merge into the two (blue) edges in (c). Note that in this edge collapse operation, five edges are transformed into two. The operator is prioritized by the feature values of an edge, thereby allowing the network to select which parts of the mesh to simplify, and which to leave intact. This creates a task-aware process, where the network learns to determine object part importance with respect to its mission (see Figure 3).

4 METHOD

MeshCNN receives as input two tensors, \mathcal{F} and \mathcal{N} , which describe the features (\mathcal{F}) and neighbors (\mathcal{N}) per edge. The combination of \mathcal{F} and \mathcal{N} enable construction of a regular matrix upon which the convolution operation is applied. When \mathcal{F} is first constructed, it is filled with the values of various geometric features computed on the edges, such as the dihedral angle, opposite angles and the ratio between the edge length and the length of its perpendicular line (shown in Figure 5). The second tensor, \mathcal{N} , is an auxiliary matrix that marks the receptive field of each edge, by storing the unique identifiers of the neighbors of an edge in the corresponding edge row. During convolution, \mathcal{N} essentially exposes the sub-matrices of \mathcal{F} that must participate in the operation. During the first convolution operation the convolution kernel is applied on the input features (shown in Figure 5), and outputs the learned feature activation maps. From this point on, the initial input geometric features have been abstracted to learned features (similar to RGB pixel values in image CNNs). As implied by the grid form of our input, MeshCNN assumes and expects a fixed number of neighbors per edge. A manifold mesh is the ideal configuration in this scenario, as each edge is guaranteed to be incident to at most two faces, thus the number of edge neighbors is at most four. To this end, we opt to constrain our input meshes to manifolds, and transform any invalid, non-manifold instance, to a valid form by locating all non-manifold edges and removing all their incident faces. Note that a manifold mesh may contain boundary edges, which are incident to only one face. Boundary edges have only two neighboring edges, which we zero pad in the convolution operation.

Following the output of the convolution layer, we apply batch-norm [Ioffe and Szegedy 2015] and relu [Nair and Hinton 2010] to the feature activation maps before reaching the pooling operation. Similar to traditional CNN pooling, our mesh pooling operation downsamples the resolution of the feature activation maps to a predefined number of edges, reducing the number of subsequent computations and emphasizing and strengthening the learned features specific to the task at hand (*i.e.*, the network loss). The edges list and their features are the input to the pooling operator (shown in Figure 5); edges are prioritized based on the magnitude of their features. The edges with minimum magnitude are candidates for deletion, each such edge is collapsed, merging the two adjacent faces (see Figure 4). This results in a global pooling, where the network is able to non-uniformly discard irrelevant sections of the mesh. This is important since if a mesh is highly triangulated in a specific region which is irrelevant to the network loss function, the pooling operation can collapse unimportant regions non-uniformly. Therefore, we have given the ability to the network to decide which regions are important to preserve - leading to a task-driven pooling operation.

Finally, defining a sequence of mesh convolution, normalization, non-linear activation and pooling layers forms a generalized network for performing any task given the relevant data and loss function (for example segmentation or classification).

In what follows, we expand and provide details about our mesh convolution and mesh pooling operations.

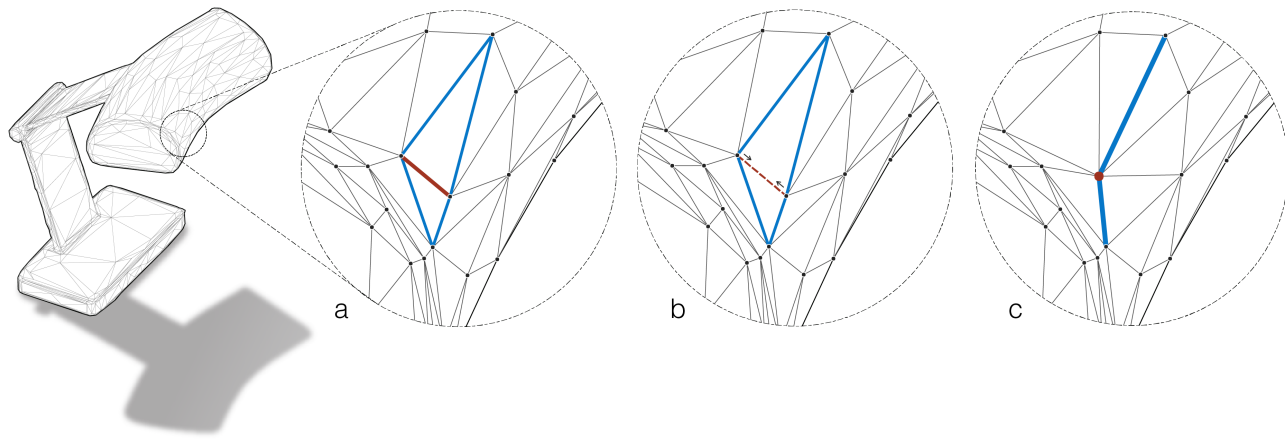


Fig. 4. (a) Features are computed on the edges by applying convolutions with neighborhoods made up of the four edges of the two incident triangles of an edge. The four blue edges are incident to the edge in red. (b) and (c) demonstrate a pooling step. In (b), the red edge is collapsing to a point, and the four incident (blue) edges collapse into the two (blue) edges in (c). Note that in an edge collapse step, five edges are converted into two.

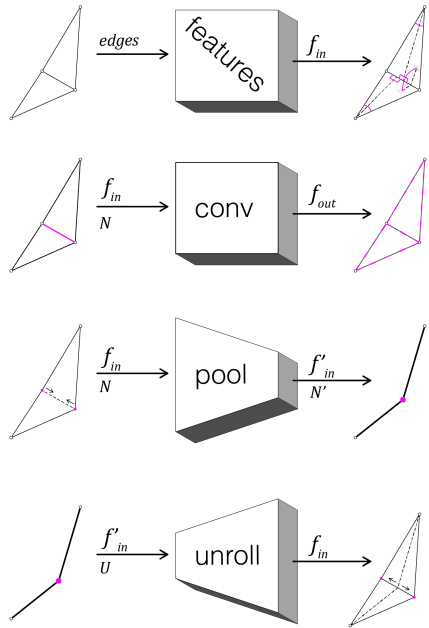


Fig. 5. Each of the building blocks implemented in MeshCNN. *features*: takes a list of edges and converts them into a 6-dimensional feature (the dihedral angle, two inner angles, two edge-length ratios for each face and one global edge length ratio). *conv*: takes a list of features and N (a matrix of indices describing the edge neighbors) used to define the convolution. *pool*: takes the edge features and reduces them by simplification and updating the neighbors. *unroll*: history for where each collapsed edge came from in the original list.

4.1 Mesh Convolution

Standard CNNs perform convolutions in fixed sized neighborhoods across a grid. Analogous to that process, in MeshCNN, we define the neighborhood around an edge to be its 1-ring neighbors, as mentioned above. To determine a consistent neighbor ordering, we follow the ordering implied by the incident face normal.

For every edge in the mesh, the adjacent neighbors are aggregated into the neighborhood matrix N . The dimensions of N are: $b \times e \times n$, where b is the batch size, e is a predefined maximum number of edges (per mesh), and n is the number of neighbors (in the case of a 1-ring convolution $n = 4$). The feature for each edge is stored in \mathcal{F} with dimensions $b \times e \times c$, where b and e are again the batch size and number of edges, and c is channel dimension (number of features).

Recall that convolution of a multi-channel image with a kernel can be implemented with general matrix multiplication (*GEMM*): by expanding (or *unwrapping*) the image into a column matrix (*i.e.*, *im2col*). Equivalently, we build an unwrapped matrix to perform the convolution operation.

In practice, we use *conv2D* since it is highly optimized. Using \mathcal{F} and N we construct a generalized edge-image matrix called I_e . Using the same notation as previously, this matrix has dimensions $b \times c \times e \times n$. Defining a generalized edge-image matrix in this way now enables use of regular 2D convolution to convolve $(5, 1)$ kernels (the four adjacent neighbors plus the central edge itself). The convolution parameters are then defined as being k kernels of size $(n + 1, 1)$. Note that since we have already padded I_e with zeros where necessary, the convolution padding is 0 (or in other words *valid*). Now the $(5, 1)$ kernel parameters will slide across the edge-image matrix, given the neighbors defined by the topology. Following convolution, a new feature tensor \mathcal{F}' is generated, where the dimension of the number of features f is now equal to k (just as in images). Note that after each pooling phase, a new N' will be generated which will define new neighbors for each subsequent convolution.

4.2 Mesh Pooling

We extend conventional pooling to irregular data, by identifying three core operations that together generalize the notion of pooling:

- 1) define pooling region given adjacency
- 2) merge features in each pooling region
- 3) redefine adjacency for the merged features

When performing pooling on regular data such as images, adjacency is inherently implied and, accordingly, the pooling region is determined directly by the chosen kernel size. Since features in each region are merged (e.g., via *max*) in a way that yields another uniformly spaced grid, the new adjacency is once again inherently defined. Having addressed the three general pooling operations defined above, it is evident that conventional pooling is a special case of the generalized process.

Mesh pooling is another special case of generalized pooling, where adjacency is determined by the topology. In runtime, extracting mesh adjacency information (e.g., edge neighbors) requires querying special data structures which are continually updated (see Section 5.2 for details).

Our pooling receives as input a tensor of edge features \mathcal{F} and a data structure \mathcal{M} with the mesh elements. First, the edge feature with the *minimum* magnitude is selected for collapse (deletion), called the *minimum edge*. Note that each collapse is a *global* search over all edge features in each mesh, which enables the network to non-uniformly collapse certain regions which are least important to the loss. Recall that collapsing an edge which is adjacent to two faces results in a deletion of three edges (shown in Figure 4), since both faces become a single edge. Each face contains three edges: the minimum edge and two adjacent neighbors of the minimum edge (see minimum edge in red and adjacent neighbors in blue in Figure 4). Each of the features of the three edges in each face are merged into a new edge feature by taking the *max* (or average) over each feature channel. First, the index of the minimum edge e^* is given by:

$$e^* = \min_{\forall i \in e} \sqrt{\sum_{j=1}^c \mathcal{F}(e_i, c_j)^2}, \quad (1)$$

then the merge operation is

$$\mathcal{F}(\text{adj} < e^*, 1|T_n>, c_j) = \max \begin{cases} \mathcal{F}(e^*, c_j) \\ \mathcal{F}(\text{adj} < e^*, 1|T_n>, c_j) \\ \mathcal{F}(\text{adj} < e^*, 2|T_n>, c_j) \end{cases}, \quad (2)$$

where $\text{adj} < e^*, 1|T_n>$ and $\text{adj} < e^*, 2|T_n>$ are the indices of the first and second neighbor of e^* (given triangular face T_n) respectively, and c_j is the feature channel index. After edge collapse, the corresponding mesh data-structures must be updated for the subsequent edge collapses (see Section 5.2 for details).

Finally, note that not every edge can be collapsed. An edge collapse yielding a non-manifold face is not allowed in our setting, as it violates the structure of \mathcal{N} . Therefore, an edge is considered invalid to collapse if it has three vertices on the intersection of its 1-ring, or if it has two boundary vertices.

5 IMPLEMENTATION DETAILS

5.1 Mesh Data Augmentation

Several forms of data augmentation exist for generating more data samples for the network. In order to be robust to different meshings, we create several different triangulations of the same object. Note since our input features are invariant to rotation, translation and isotropic scaling (same in x , y and z) - these augmentations would not generate new input features. However, we can generate different features via anisotropic scaling on the vertex locations in x , y and z $< S_x, S_y, S_z >$ which will change the input features to the network.

5.2 Mesh Data Structures

In practice, we keep tabs of the identity of the merged edges, and perform feature concatenation for the corresponding edges in several big swoops. This bookkeeping can also be used to unroll the collapse operations for tasks such as segmentation computation.

Since pooling changes the structure of the mesh, not only does the matrix \mathcal{F} require an update, but also the neighborhood matrix \mathcal{N} , in preparation for the next convolution layer. To this end, data structures are maintained during this operation. A priority queue determines edge collapse order and a union-find structure holds all subgroups of merged edges that can later be used for unroll operations. A vertex-edge adjacency list and boundary edge list are constantly maintained for validation of edge collapse operations and for faster updates of \mathcal{N} . Finally, The original vertices and faces sets are maintained in order to support reconstruction of the mesh, but can be waived during training.

6 EXPERIMENTS

Using the MeshCNN building blocks described in Section 4, we can construct different network configurations for the purpose of solving different tasks. Conventionally, designing traditional CNNs to undertake a particular task (e.g., classification) consists of defining both the number of convolution, pooling and fully-connected layers (*network depth*) in addition to the number of parameters in each layer (*network width*). Likewise, the building blocks of MeshCNN provide an analogous *plug-and-play* framework. In the following subsections, we use the MeshCNN building blocks on the tasks of classification and segmentation.

6.1 3D Mesh Classification

To better illustrate the distinctive power of MeshCNN, we modeled a large set of cubes and engraved icons in one side of each cube (see Figure 6). The cube tessellation is non-uniform, where five faces are modeled by two large triangles and one face contains fine grained features, modeled by a large number of small triangles that connect to the engraved icon. Certainly, modeling these cubes with point clouds requires a large number of evenly distributed points across the large faces of the cubes (see Figure 7).

There are ten classes of engraved cubes, grouped by the identity of the icon. The networks, PointNet [Qi et al. 2017a] and MeshCNN were trained to classify the cubes. Table 6 shows that with only a fraction of the capacity (*model weights*), MeshCNN achieves drastically higher test accuracy. While this example may be considered contrived, it is meant to highlight that MeshCNN excels on 3D

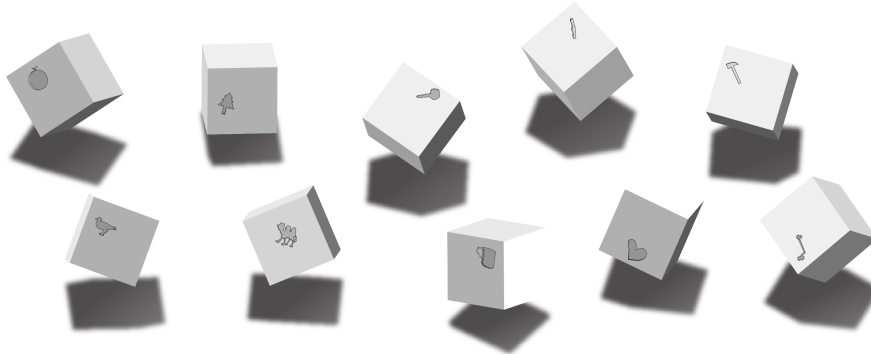


Fig. 6. Engraved cubes dataset used to evaluate mesh classification. We generate 10 different classes by extruding stickers from MPEG-7 [Latecki and Lakamper 2000], and placing them on a random face in a random location.

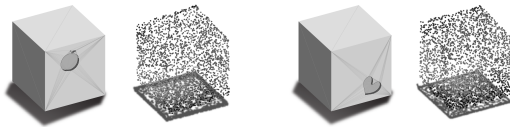


Fig. 7. An example of two different classes (*apple* and *heart*) in the mesh and pointcloud form. While it is immediately obvious which mesh belongs to the *heart* or *apple* class, the two pointcloud samples appear indistinguishable.

3D Mesh Classification			
method	input dim	capacity	test acc
MeshCNN	1300	0.255M	91.2%
PointNet	2500	1.61M	21.8%
PointNet	5000	1.61M	25.0%

Table 1. Results on engraved cubes (shown in Figure 6). MeshCNN is able to significantly out-perform PointNet, using 85% less features

shapes that contain regions that can be modeled with a rather small number of large triangles.

We also show that MeshCNN can handle a global high-level classification task on shapes with uniformly sized triangles. To this end, we remesh the engraved cube shapes to give a uniform distribution of triangles (namely adding more triangles to the flat cube surface). Using the uniformly triangulated meshes, we trained the 10-class classification network. The resolution of the input mesh starts at at most 750 edges, with a series of 4 mesh convolution and mesh pooling layers that iteratively collapse to $660 \rightarrow 510 \rightarrow 360 \rightarrow 210$ target edges. To visualize the effect of the mesh-pooling on the classification task, we extracted the intermediate results following each mesh pooling operation (shown in Figure 8). Observe how MeshCNN learned to reduce the edges irrelevant to the classification task (flat cube surfaces) while preserving the edges within and surrounding the icon engraving.

6.2 3D Mesh Segmentation

Another central application of MeshCNN is consistent shape segmentation, which is an important building block for many applications in shape analysis and synthesis. We used supervised learning to train MeshCNN to predict, for every edge, the probability of belonging to a particular segment. First, we simplified each mesh to *roughly* the same number of edges and generated several different triangulations for each sample. Note that as mentioned earlier, our MeshCNN does not require the same number of edges across all samples. We used the COSEG [2012] dataset which provides ground truth segmentation as a label per face. We generated edge-level semantic labeling on the simplified meshes based on the labels from the original resolution. The most straightforward MeshCNN semantic segmentation configuration would be to use a sequence of mesh convolution layers (along with normalization and non-linear activation units). However, incorporating mesh pooling enables MeshCNN to learn a segmentation-driven edge collapse, learning to merge edges from the same segment while preserving boundary edges. Recall that mesh pooling reduces the input mesh resolution, which is no longer consistent with the ground-truth edge-level labels. To overcome this, the final network layer is an *unroll* layer (see Figure 5). This layer takes the pooled meshes and *unrolls* it into the resolution of the input mesh based on the collapse history. Note that while the unroll layer is differential, it does not contain any learnable parameters. The final segmentation predictions from MeshCNN semantic segmentation network with pooling and unrolling layers on a (held out) test set is shown in Figure 9.

7 DISCUSSION AND FUTURE WORK

In this paper, we presented MeshCNN, a neural network that learns and directly analyzes shapes in mesh form. The key contribution of our work is the definition and application of convolution and pooling operations tailored for irregular and non-uniform structures. We demonstrate this ability over edge features and triangular meshes, however, similar constructs can be designed for face features as well as for quad meshes. Our choice of mesh edges as basic building blocks upon which the network operates, is of great importance, as the edge set dictates a simple means to define a local, fixed sized



Fig. 8. MeshCNN trained to predict the class of icon engraving with uniform sized triangles. Left: input mesh (test set) at full resolution (at most) 750 edges passed through 4 series of mesh convolutions and mesh pooling. From (second) left to right, are the output meshes from the four pooling layers with target edges: 660 \rightarrow 510 \rightarrow 360 \rightarrow 210. Observe how the network learns to preserve important edges and remove redundant edges with regards to the classification task.



Fig. 9. Semantic segmentation results on (held out) test shapes. MeshCNN uses mesh pooling to learn to collapse edges from the same segments, which are unrolled back to the original input mesh resolution via the mesh unroll layer.

neighborhood for convolutions over irregular structures. Additionally, pooling operations are carried out by edge collapse in a global manner based on the learned edge features, leading to task-driven pooling driven by the networks loss function.

We demonstrated that by leveraging these features, MeshCNN learns which edges to collapse based on the given task. This is an important contribution with the potential to influence many image-based CNN tasks, e.g., high resolution image segmentation typically produces a low resolution segmentation map and upsamples it, possibly with skip connections. The pooling in MeshCNN simplifies (semantically) uniform regions while preserving complex ones; therefore, in the future, we are interesting in applying a global pooling on image segmentation to obtain a high resolution segmentation map (without needing to upsample a low-resolution image). In this application, large uniform regions from the same segmentation class will be represented by a small number of pixels, while keeping the boundaries at the original resolution. Finally, in this work, deep features are leveraged both for obvious task solving purposes, but also for edge collapse guidance. In the future, we are interested in splitting our features into two forms consisting of "task features" and "simplification features", in a divide-and-conquer attempt to achieve better specialization of the learned features.

Our current work focuses on the fundamentals of learning on triangular meshes. In the near future, we would like to continue and further develop the un-pooling and de-convolution operators, and

in general provide up-sampling layers over triangular meshes for the development of auto-encoders for meshes. Mesh upsampling via vertex-split can be performed by reversing the order of the edge collapse operations by bookkeeping the list of edge collapses performed earlier. This is similar to the bookkeeping that is used for the unroll layer. When synthesizing new meshes, we let the network decide which vertex to split, again by splitting vertices that are adjacent to edges with high feature values.

REFERENCES

James Atwood and Don Towsley. 2016. Diffusion-Convolutional Neural Networks. In *Advances in Neural Information Processing Systems (NIPS)*.

Davide Boscaini, Jonathan Masci, Emanuele Rodola, and Michael Bronstein. 2016. Learning shape correspondence with anisotropic convolutional neural networks. In *Advances in Neural Information Processing Systems*. 3189–3197.

Mario Botsch, Leif Kobbelt, Mark Pauly, Pierre Alliez, and Bruno Lévy. 2010. *Polygon mesh processing*. AK Peters/CRC Press.

Andrew Brock, Theodore Lim, J.M. Ritchie, and Nick Weston. 2016. Generative and Discriminative Voxel Modeling with Convolutional Neural Networks. In *NIPS 3D Deep Learning Workshop*.

Michael M. Bronstein, Joan Bruna, Yann LeCun, Arthur Szlam, and Pierre Vandergheynst. 2017. Geometric Deep Learning: Going beyond Euclidean data. *IEEE Signal Process. Mag.* 34, 4 (2017), 18–42. <https://doi.org/10.1109/MSP.2017.2693418>

Joan Bruna, Wojciech Zaremba, Arthur Szlam, and Yann LeCun. 2014. Spectral Networks and Locally Connected Networks on Graphs. In *International Conference on Learning Representations (ICLR)*.

Liang-Chieh Chen, George Papandreou, Iasonas Kokkinos, Kevin Murphy, and Alan L Yuille. 2018. DeepLab: Semantic image segmentation with deep convolutional nets, atrous convolution, and fully connected crfs. *IEEE transactions on pattern analysis and machine intelligence* 40, 4 (2018), 834–848.

Michael Garland and Paul S Heckbert. 1997. Surface simplification using quadric error metrics. In *Proceedings of the 24th annual conference on Computer graphics and interactive techniques*. ACM Press/Addison-Wesley Publishing Co., 209–216.

Benjamin Graham, Martin Engelcke, and Laurens van der Maaten. 2017. 3D Semantic Segmentation with Submanifold Sparse Convolutional Networks. *CoRR* abs/1711.10275 (2017).

Rana Hanocka, Noa Fish, Zhenhua Wang, Raja Giryes, Shachar Fleishman, and Daniel Cohen-Or. 2018. ALIGNet: Partial-Shape Agnostic Alignment via Unsupervised Learning. *arXiv preprint arXiv:1804.08497* (2018).

Mikael Henaff, Joan Bruna, and Yann LeCun. 2015. Deep Convolutional Networks on Graph-Structured Data. *CoRR* abs/1506.05163 (2015).

Hugues Hoppe. 1997. View-dependent refinement of progressive meshes. In *Proceedings of the 24th annual conference on Computer graphics and interactive techniques*. ACM Press/Addison-Wesley Publishing Co., 189–198.

Hugues Hoppe, Tony DeRose, Tom Duchamp, John McDonald, and Werner Stuetzle. 1993. Mesh optimization. In *Proceedings of the 20th annual conference on Computer graphics and interactive techniques*. ACM, 19–26.

Sergey Ioffe and Christian Szegedy. 2015. Batch normalization: Accelerating deep network training by reducing internal covariate shift. *arXiv preprint arXiv:1502.03167* (2015).

Longin Jan Latecki and Rolf Lakamper. 2000. Shape similarity measure based on correspondence of visual parts. *IEEE Transactions on Pattern Analysis and Machine Intelligence* 22, 10 (2000), 1185–1190.

J. Li, K. Xu, S. Chaudhuri, E. Yumer, H. Zhang, and L. Guibas. 2017. GRASS: Generative Recursive Autoencoders for Shape Structures. *ACM Transactions on Graphics*

(*Proceedings of SIGGRAPH 2017*) (2017).

Yangyan Li, Rui Bu, Mingchao Sun, and Baoquan Chen. 2018. PointCNN. *CoRR* abs/1801.07791 (2018).

Yangyan Li, Soren Pirk, Hao Su, Charles R Qi, and Leonidas J Guibas. 2016. FPNN: Field probing neural networks for 3D data. In *Advances in Neural Information Processing Systems (NIPS)*. 307–315.

Haggai Maron, Meirav Galun, Noam Aigerman, Miri Trope, Nadav Dym, Ersin Yumer, Vladimir G Kim, and Yaron Lipman. 2017. Convolutional neural networks on surfaces via seamless toric covers. *ACM Trans. Graph.* 36, 4 (2017), 71.

Jonathan Masci, Davide Boscaini, Michael Bronstein, and Pierre Vandergheynst. 2015. Geodesic convolutional neural networks on riemannian manifolds. In *Proceedings of the IEEE international conference on computer vision workshops*. 37–45.

Vinod Nair and Geoffrey E Hinton. 2010. Rectified linear units improve restricted boltzmann machines. In *Proceedings of the 27th international conference on machine learning (ICML-10)*. 807–814.

Mathias Niepert, Mohamed Ahmed, and Konstantin Kutzkov. 2016. Learning Convolutional Neural Networks for Graphs. In *International Conference on Machine Learning (ICML)*.

Charles R Qi, Hao Su, Kaichun Mo, , and Leonidas J Guibas. 2017a. PointNet: Deep Learning on Point Sets for 3D Classification and Segmentation. In *Computer Vision and Pattern Recognition (CVPR)*. 77–85.

Charles R Qi, Hao Su, Kaichun Mo, and Leonidas J Guibas. 2017b. Pointnet: Deep learning on point sets for 3d classification and segmentation. *Proc. Computer Vision and Pattern Recognition (CVPR), IEEE* 1, 2 (2017), 4.

Charles R. Qi, Hao Su, Matthias Niessner, Angela Dai, Mengyuan Yan, and Leonidas J. Guibas. 2016. Volumetric and multi-view CNNs for object classification on 3d data. In *Computer Vision and Pattern Recognition (CVPR)*. 5648–5656.

Charles R. Qi, Li Yi, Hao Su, and Leonidas J. Guibas. 2017. PointNet++: Deep Hierarchical Feature Learning on Point Sets in a Metric Space. In *Advances in Neural Information Processing Systems (NIPS)*. 5105–5114.

Gernot Riegler, Ali Osman Ulusoy, and Andreas Geiger. 2017. OctNet: Learning deep 3D representations at high resolutions. In *Computer Vision and Pattern Recognition (CVPR)*.

Pierre Sermanet, David Eigen, Xiang Zhang, Michaël Mathieu, Rob Fergus, and Yann LeCun. 2013. Overfeat: Integrated recognition, localization and detection using convolutional networks. *arXiv preprint arXiv:1312.6229* (2013).

Karen Simonyan and Andrew Zisserman. 2014. Very deep convolutional networks for large-scale image recognition. *arXiv preprint arXiv:1409.1556* (2014).

Ayan Sinha, Jing Bai, and Karthik Ramani. 2016. Deep learning 3D shape surfaces using geometry images. In *European Conference on Computer Vision*. Springer, 223–240.

Hang Su, Subhransu Maji, Evangelos Kalogerakis, and Erik Learned-Millers. 2015. Multi-view Convolutional Neural Networks for 3D Shape Recognition. In *International Conference on Computer Vision (ICCV)*.

F. P. Such, S. Sah, M. A. Dominguez, S. Pillai, C. Zhang, A. Michael, N. D. Cahill, and R. Ptucha. 2017. Robust Spatial Filtering With Graph Convolutional Neural Networks. *IEEE Journal of Selected Topics in Signal Processing* 11, 6 (Sept 2017), 884–896.

Maxim Tatarchenko, Jaesik Park, Vladlen Koltun, and Qian-Yi Zhou. 2018. Tangent Convolutions for Dense Prediction in 3D. In *Proceedings of the IEEE Conference on Computer Vision and Pattern Recognition*. 3887–3896.

Lyne P. Tchapmi, Christopher B. Choy, Iro Armeni, JunYoung Gwak, and Silvio Savarese. 2017. SEGCloud: Semantic Segmentation of 3D Point Clouds. In *3DV*.

Peng-Shuai Wang, Yang Liu, Yu-Xiao Guo, Chun-Yu Sun, and Xin Tong. 2017. O-CNN: Octree-based Convolutional Neural Networks for 3D Shape Analysis. *ACM Trans. Graph.* 36, 4, Article 72 (July 2017), 11 pages. <https://doi.org/10.1145/3072959.3073608>

Yunhai Wang, Shmulik Asafi, Oliver van Kaick, Hao Zhang, Daniel Cohen-Or, and Baoquan Chen. 2012. Active co-analysis of a set of shapes. *ACM Transactions on Graphics (TOG)* 31, 6 (2012), 165.

Yue Wang, Yongbin Sun, Ziwei Liu, Sanjay E Sarma, Michael M Bronstein, and Justin M Solomon. 2018. Dynamic Graph CNN for Learning on Point Clouds. *arXiv preprint arXiv:1801.07829* (2018).

Zhirong Wu, Shuran Song, Aditya Khosla, Fisher Yu, Linguang Zhang, Xiaoou Tang, and Jianxiong Xiao. 2015. 3D shapenets: A deep representation for volumetric shapes. In *Computer Vision and Pattern Recognition (CVPR)*. 1912–1920.